Multi-drug tolerance in *Leishmania* persister-like cells

Allison Aroni-Soto[1,2,5], Pieter Monsieurs[1,5], Odin Goovaerts[3], Kaoutar Choukri[1,5], Basudha Khanal[4], Wim Adriaensen[3], Jean-Claude Dujardin[2, 5], Michael P. Barrett[6], Malgorzata A. Domagalska[1,5*]

[1] Institute of Tropical Medicine, Experimental Parasitology Unit, Antwerp, Belgium
[2] Department of Biomedical Sciences, University of Antwerp, Belgium
[3] Institute of Tropical Medicine, Clinical Immunology Unit, Antwerp, Belgium
[4] Department of Microbiology, BP Koirala Institute of Health Sciences, Dharan, Nepal
[5] Institute of Tropical Medicine, Molecular Parasitology Unit, Antwerp, Belgium
[6] School of Infection & Immunity, College of Medical, Veterinary and Life Sciences, University of Glasgow, Glasgow, UK

***Correspondence:**
Malgorzata A. Domagalska: mdomagalska@itg.be

Keywords: *Leishmania*, persisters, quiescence, multi-drug tolerance

Abstract

Leishmaniasis is caused by parasitic protozoa of the genus *Leishmania* and is found widely across the tropics and sub-tropics, afflicting hundreds of thousands of people. The disease is notoriously difficult to treat. Here, we present evidence of the existence of persister-like cells in cultured *Leishmania* populations, induced upon exposure to normally lethal doses of antimony, a widely used anti-leishmanial. Persisters are a small fraction of non-proliferative cells with reduced metabolism that are adapted to withstand a variety of environmental assaults, including lethal doses of antimicrobials. We show that *Leishmania* persister-like cells survive lethal doses of antimonials by adopting a quiescence phenotype characterised by reduced proliferation, constrained metabolism, and diminished mitochondrial membrane potential. What is more, these cells demonstrate cross-tolerance to other anti-leishmanial drugs. Wild-type persister-like cells reverted to similar levels of drug susceptibility once the antimony-induced pressure was removed. Surprisingly, cells which had previously been selected for genetic changes causing resistance to antimony acquired a level of hyper-resistance after transient passage through the quiescent state, without further genetic change. Our results demonstrate the extreme versatility of this eukaryotic pathogen in adaptation to drug pressure and highlight the need for the development of new anti-leishmanials targeting non-proliferative forms.

38 **Main**

39 The ability of microorganisms to resist the killing action of antimicrobial agents is emerging as one
40 of the most serious public health threats and has been observed for antivirals, antibiotics, antifungals,
41 and also antiparasitic compounds [1]. Understanding the mechanisms that allow them to survive
42 chemotherapy is essential. Several molecular mechanisms can underlie this phenomenon, but the most
43 extensively studied one is drug resistance caused by acquired, heritable genetic changes, usually point
44 mutations or insertion/deletion within genes in which these mutations enable cells to prevent the
45 drug's toxic capacity [2,3]. Importantly, resistant pathogens remain metabolically active and can grow and
46 replicate in the presence of drugs. However, microorganisms can also adopt a physiological state of
47 transient quiescence, manifested by non-proliferation and reduced metabolism. This leads to non-
48 heritable drug tolerance in cases where drug activity depends upon metabolic activities suppressed in
49 quiescence [4]. This can affect whole-microbial populations, but heterogeneity within microbial
50 populations may allow the survival of a small number of specialized quiescent cells, termed 'persisters',
51 in the presence of an antimicrobial agent [5]. After the removal of drug pressure, persisters resume
52 growth and switch back to their drug-sensitive phenotype. The presence of persisters is of particular
53 importance as their quiescent phenotype associated with exposure to a single drug often leads to
54 multidrug tolerance [6–8].

55 Quiescence is a non-proliferative, physiological resting state that can be adopted by many
56 infectious microorganisms, including bacteria, fungi, and some protozoan parasites as a strategy to
57 survive nutrient limitation, host immunity, and chemotherapy [9]. This reversible state is characterized
58 by an active and regulated cellular and molecular remodelling programme resulting in reduced
59 metabolism, transcription, and translation [9,10]. Importantly, while overall metabolism is switched into
60 an energy-saving mode, crucial processes allowing the survival of the cells under stress conditions
61 remain active, and some processes are even selectively upregulated in the quiescent state [11].

62 *Leishmania* are digenetic protozoan parasites that cycle between the sand fly vector and
63 mammalian host. They cause a spectrum of diseases, the most severe form being visceral leishmaniasis
64 (VL), which is lethal if left untreated. *Leishmania donovani* is the etiological agent of VL in the Indian
65 subcontinent (ISC) and in East Africa. Antimonials (Sb) were the first drugs used in the treatment of VL,
66 but they have been replaced first by miltefosine and later by Amphotericin B (AmB) in the ISC due to
67 loss of efficacy attributed to the emergence of drug resistance [12–15]. Phylogenomic analysis of 204 *L.*
68 *donovani* isolates, followed by experimental studies allowed the identification and characterization of
69 different genomic pre-adaptations to antimonials in *Leishmania* in the ISC [16]. They identified i) a small
70 group of ISC1 parasites, which diverged early and have no obvious genomic pre-adaptation to
71 antimony, ii) a dominant, so-called core group of parasites consisting of several closely related lineages
72 which are pre-adapted to antimony through either the presence of the intra-chromosomal
73 amplification of the H-locus, which contains the MRPA gene, a known driver of antimony resistance or
74 iii) another group with increased H-locus copy number, plus a 2-nt insertion in the AQP1 gene (ISC5),
75 that encodes a key importer of antimony whose loss also contributes to resistance to the drug [16,17].

76 In terms of drug responses in *Leishmania,* most research has focused on identification of potential
77 drug resistance signatures in natural populations and in experimental evolution studies [16,18–21].
78 However, recent evidence points to the existence of quiescence and its role in adaptation to drug
79 pressure [22–26]. Quiescence in *Leishmania* was inferred in mice when amastigotes of *L. mexicana* were
80 shown to have a very low replication rate, together with low rates of RNA synthesis, protein turnover,

and membrane lipid synthesis [27]. Another mouse study revealed heterogeneity among *L. major* amastigotes with non-replicating parasites distinguished from slowly replicating populations [28]. Another study of *L. mexicana* in mice revealed quiescent populations within collagen-rich mesothelium surrounding lesions, where miltefosine accumulation was also limited [25]. Using an in vitro antimony-exposure model, we showed that *L. lainsoni* parasites exhibit hallmarks of a quiescence state and that drug-tolerant and persister-like cells of genetically diverse strains of *L. braziliensis* could be detected under high doses of potassium antimonium tartrate (PAT) [23,24]. Recently, Dirkx and colleagues showed that long-term hematopoietic stem cells provide a parasite niche during treatment failure in an animal model of VL infection [29]. Bone marrow stem cell-associated parasites were proposed to enter into quiescence after 2-3 replication cycles with parasites emerging post-quiescence with increased apparent infectivity [26].

In selecting drug resistance in laboratory studies in *Leishmania*, it has become clear that these organisms have particularly plastic genomes and hundreds of karyotypes can emerge from a single clonal population grown in culture [17,21,30–32]. This phenomenon, termed mosaic aneuploidy, is postulated to underlie phenotypic heterogeneity and facilitate adaptation to changing environmental conditions, including drug pressure [32,33]. Generally, persisters in bacteria do not emerge due to genetic changes, however, it is important to ascertain whether a similar process relates to quiescence in *Leishmania* in the selection of drug-tolerant persister-like cells.

In this study, we addressed: i) the role of quiescence and population heterogeneity in the survival of *L. donovani* promastigotes under normally lethal doses of PAT, and ii) whether the presence of genomically defined pre-adaptations to antimony has an impact on the quiescence and persister phenotypes under PAT exposure. We found compelling evidence that quiescence is a universal survival mechanism adapted by genomically distinct *L. donovani* strains. However, the impact of the transition through quiescence, on drug susceptibility differed, depending on the presence of genomic pre-adaptations to antimony. In non-preadapted parasites, the antimony tolerance phenotype was reversible in non-drug conditions. In contrast, in resistant parasites a small sub-population of persisters gave rise to a population of parasites with further increased resistance to antimony. The quiescent state observed in both types of persister-like cells can provide tolerance to PAT, but also other antileishmanial compounds. With this study, we demonstrate for the first time multidrug tolerance in persister-like cells of a eukaryotic pathogen.

Results

Isogenic *L. donovani* lines exposed to normally lethal doses of PAT exhibit intrinsic population heterogeneity in their drug susceptibility

To address whether heterogeneity within populations and quiescence plays a role in response to drug pressure in *L. donovani*, we developed an experimental model, in which we focused on the detection of a small subpopulation of surviving persister-like cells. Specifically, we aimed to identify cells that i) constituted a small subpopulation within isogenic lines, ii) could survive in the presence of a normally lethal dose of a drug and iii) showed a reduction in growth and metabolism associated with quiescent state when compared with the majority of cells. We chose trivalent antimony (PAT), as we showed previously that quiescent cells could be observed in the presence of high doses of this drug in a dermotropic species of *Leishmania*, *L. braziliensis* [23].

We selected ten cloned strains of *L. donovani* isolated in the ISC, with different levels of genomic pre-adaptation to antimony: i) three strains where no obvious genomic changes indicative of pre-adaptation to PAT resistance are known to be present (ISC1); these strains are highly susceptible to PAT; ii) seven strains belonging to different genetic groups (ISC4, 6, and 9) characterized by possessing one known genomic pre-adaptation to PAT, the intra-chromosomal amplification of the H-locus, which contains the MRPA gene, a known driver of antimony resistance; these strains show decreased susceptibility to PAT; iii) one strain with two known genomic pre-adaptations to PAT: a 2-nt insertion in the AQP1 locus, proposed to be associated with antimonial resistance observed in the ISC5 genotype in addition to the intra-chromosomal amplification of the H-locus; the strain shows a low susceptibility to PAT [16,17]. We also included a reference *L. donovani* strain isolated in East Africa (LdBob), highly susceptible to antimony (Table 1) [34,35]. Of note, one of the strains belonging to ISC6 group, BPK085 also carries a different 2-nt insertion mutation in the AQP1 locus, which results in a frameshift [16].

Table 1. Cloned strains of *L. donovani* isolates from the Indian Subcontinent and reference strain (LdBOB) used in this study.

Strain	ISC population	H-locus amplified	AQP1 indel†
Profile 1*			
BPK026	ISC1	no	no
BPK031	ISC1	no	no
BPK156	ISC1	no	no
Profile 2*			
BPK190	ISC4	yes	no
BPK087	ISC4	yes	no
LdBOB	Other	no	no
Profile 3*			
BPK085	ISC6	yes	no
BPK282	ISC6	yes	no
BPK294	ISC9	yes	no
Profile 4*			
BPK080	ISC4	yes	no
BPK275	ISC5	yes	yes

* Profiles 1-4 correspond to patterns of survival under normally lethal PAT dose.
† Indel associated with antimonial resistance.

By using this collection of natural parasite isolates with different levels of genetic pre-adaption to antimony we aimed to study the potential interplay between different heritable, genetically defined forms of drug resistance and quiescence in parasite survival under PAT pressure. We generated rEGFP lines for each of these strains to monitor transcriptional activity of rDNA locus as a negative biomarker of quiescence during exposure to PAT [36].

In the first step, we exposed promastigotes of all lines to a range of PAT concentrations to determine for each strain, the lowest concentration (Supp. Fig.1; Supp. Table 1) at which no metabolic activity could be detected in a resazurin based assay measured at the level of the whole population [37]. By identifying normally lethal doses of PAT specific for each strain, we aimed to establish comparable experimental conditions for each strain in which physiologically quiescent-like cells would be observed, as shown for bacteria. We then subjected each line to the respective strain-specific normally lethal PAT doses over 10 days (with PAT application repeated at day 5), and we monitored viability and growth (Supp. Table 2; Supp. Fig. 2) and established the time-kill curves (Fig.1; Supp. Fig.3) during the exposure. Overall, we identified four broad viability profiles in response to PAT pressure (Fig.1; Supp. Table 2).

Profile 1 (P1) observed in the ISC1 parasites (BPK026, BPK031, BPK156) was characterized by continuous reduction of viability throughout the whole period of exposure to PAT, with the majority of the parasites killed in the first 6 days, while a small remaining population (in the range of 0.7-3.4%) was killed at a slower rate over the last 4 days, allowing those cells to persist until the end of exposure. In profile 2, P2, (BPK190, BPK087, and LdBob) we observed rapid killing of almost the entire population of cells in the first 2 days (1.8-11.0% survived beyond day 2), followed by a slower killing over the following days, with no viable parasites found by day 8. Profile 3 (P3) exhibited by BPK085, BPK282, and BPK294 could be distinguished by fast reduction in viability over the first 3-4 days reaching viability 1.9-3.4%, followed by a slower killing rate until days 6-8. Surprisingly, in the last 2 days of exposure to PAT, a clear increase in the number of viable parasites was observed reaching 5.5-14.9% at day 10. Finally, the last profile (profile 4, P4) displayed by BPK080 and BPK275 is defined by mild reduction in viability, followed by a short period of no visible growth, then a subsequent increase in the number of viable cells. BPK275, a strain with the two genomic pre-adaptations to antimony was the least affected by PAT having a viability of 70% at its lowest value (Supp. Table 2).

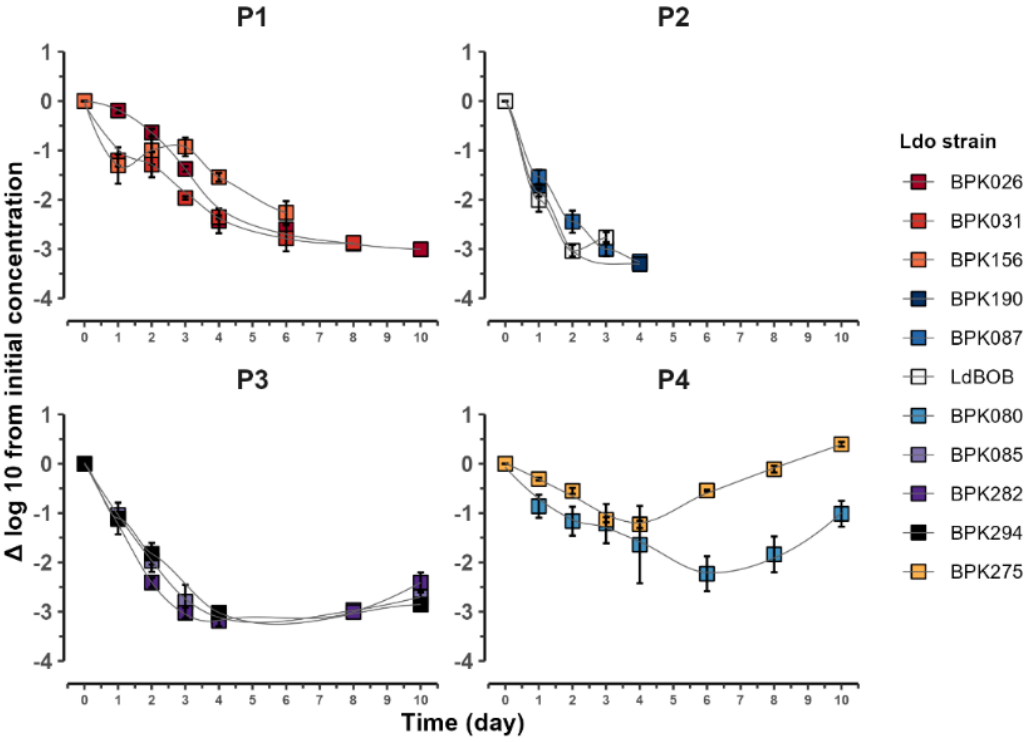

Figure 1. Patterns of survival of *L. donovani* strains under normally lethal PAT concentrations. Time-kill curves under prolonged PAT exposure (see separate strain-specific curves in Supp. Fig.2) showed four different viability profiles (Profile 1-4). Data represents the reduction in promastigote concentration relative to the initial inoculum, the viable parasites were detected by flow cytometry. The results reflect the mean ± SEM of three biological replicates.

***L. donovani* lines adopt a quiescent state to survive PAT pressure**

Given the apparent reduction in growth in all tested lines, we addressed whether the PAT-exposed cells adopt a quiescent state as a survival mechanism to prolonged drug exposure. We addressed this first by analyzing the reduction of rEGFP expression -a proxy of metabolic activity- [36] in all the lines exposed to PAT at day 2, and 4 (PAT D2 and PAT D4, respectively), as compared to proliferative promastigotes. We included, as a positive control, stationary promastigotes (No PAT D4), which are known to have properties of quiescent cells [24]. In all lines of P1/P4 we observed a progressive reduction of rEGFP under PAT pressure, reaching comparable or slightly lower levels to those observed in No PAT D4 (Fig. 2A). In parasites belonging to P2, and P3 measurements were possible only at D2 (all lines in P3 and only BPK087 in P2) due to rapid killing in the lines of these profiles, which resulted in an insufficient number of viable cells for reliable quantification of rEGFP expression. As in other lines, we detected reduction in rEGFP expression at D2 in all three P3 lines. Surprisingly, we observed an upregulation of rEGFP in BPK087 suggesting an inability to enter quiescence under PAT pressure (62.7% of increase, Fig.2A). As expected, all lines that were able to survive drug pressure, resumed normal growth after transfer to standard growth conditions without PAT (Supp. Table 3).

To confirm the quiescent status of the viable cells under PAT, we selected two lines, BPK026 and BPK275, which present the most extreme viability profiles (P1, and P4, respectively) and extreme genomic pre-adaptations to PAT (no known genomic pre-adaptations, and H-locus amplification together with the AQP1 indel associated with antimony resistance, respectively) for more in-depth

193 characterization. First, we measured daily rEGFP expression until day 7, and at the last day of PAT
194 exposure. Both lines showed an overall rEGFP decrease among viable cells over the first 4 days of PAT
195 pressure (Fig. 2B), matching the observed growth arrest (Supp. Fig. 4A). This decrease continued for
196 BPK026 over the next 6 days, reaching a value of 83.1% of reduction in expression. In contrast, rEGFP
197 expression for BPK275 remained stable until day 5, followed by a clear increase on day 10 (Fig. 2B). This
198 is consistent with the apparent reactivation and increase in the percentage of viable and proliferative
199 cells towards the end of drug exposure (Supp. Fig. 4B). Second, we assessed whether parasite
200 replication is arrested/reduced using CellTracker (tracking cell proliferation) combined with SYTOX Blue
201 dye (viability, Fig. 2C). Each round of replication dilutes the CellTracker dye resulting in decreased
202 fluorescence signal, thus fluorescence levels are expected to remain unchanged in non-proliferating
203 cells. In this assay, logarithmic promastigotes were labelled by CellTracker (D0) and either exposed to
204 PAT at a normally lethal dose (PAT) or grown in the control medium (No PAT), and the fluorescence
205 signal was evaluated during short- (D4) and long-term (D10) PAT exposure. In both lines, No PAT
206 parasites showed clear proliferation as indicated by a decrease in fluorescence, reaching 1.97 - 1.57 to
207 1.59 - 1.12 $\log_{10}$ values for BPK026 and BPK275, respectively (Fig. 2C). PAT-exposed parasites by contrast
208 showed less dilution (Fig. 2C). In BPK026, the CellTracker signal decreased slightly from 4.61 to 3.82
209 $\log_{10}$ values at PAT D4, and remained almost the same at PAT D10 (3.61 $\log_{10}$ values) indicating an overall
210 low/no proliferation of PAT-exposed cells. In the case of BPK275, the signal in PAT D4 (2.48 $\log_{10}$ values)
211 decreased as compared to D0 (4.31 $\log_{10}$ values), but it was still higher than fluorescence in the No PAT
212 D4 parasites (1.59 $\log_{10}$ values). No CellTracker signal was detected in PAT D10; this indicates that during
213 the early exposure to PAT, BPK275 parasites transiently reduce their proliferation, while resuming active
214 proliferation later.

215 Next, we investigated the mitochondrial membrane potential as an indicator of mitochondrial
216 activity, which is known to be reduced in quiescent *Leishmania* cells [24]. We labelled promastigotes at
217 different time points under PAT exposure and their respective controls, with MitoProbe™ DilC, a
218 permeable cationic dye that accumulates across the mitochondrial membrane when the interior of the
219 mitochondrion is negatively charged compared to its outside (Fig. 2D). In the absence of PAT, BPK026
220 showed high potential in logarithmic promastigotes, and this decreased significantly in the stationary
221 phase. Unexpectedly, in BPK275, the mitochondrial membrane potential was much lower in logarithmic
222 parasites in comparison to BPK026 (29,569 ± 2,071 and 10,142 ± 2147 MFI values, in BPK026 and
223 BPK275, respectively, Fig. 2D). Under PAT pressure, patterns were also markedly different between
224 lines. In BPK026, early PAT-exposed promastigotes showed a similar potential to late stationary (D10)
225 promastigotes, which further decreased to 899 ± 165 MFI values at day 10 (Fig. 2D). In the PAT-exposed
226 BPK275, the mitochondrial potential was the lowest at D2 (4,326 ± 47 MFI value), and it gradually
227 increased reaching 12,611 ± 1,741 MFI value at D10 (Fig. 2D).

228 Thus, based on the rEGFP, CellTracker, and mitochondrial potential measurements, we concluded
229 that both lines exhibited features of quiescence during their exposure to normally lethal doses of PAT.
230 Though in BPK275, the line with genetic resistance to PAT, the period of quiescence was transient, and
231 the quiescence state appeared to be less deep. The accumulated data demonstrates that although
232 different dynamics of killing could be observed in *L. donovani* promastigotes exposed to lethal doses of
233 PAT, in all lines that survived PAT pressure, adoption of a quiescent state was associated with survival.

234

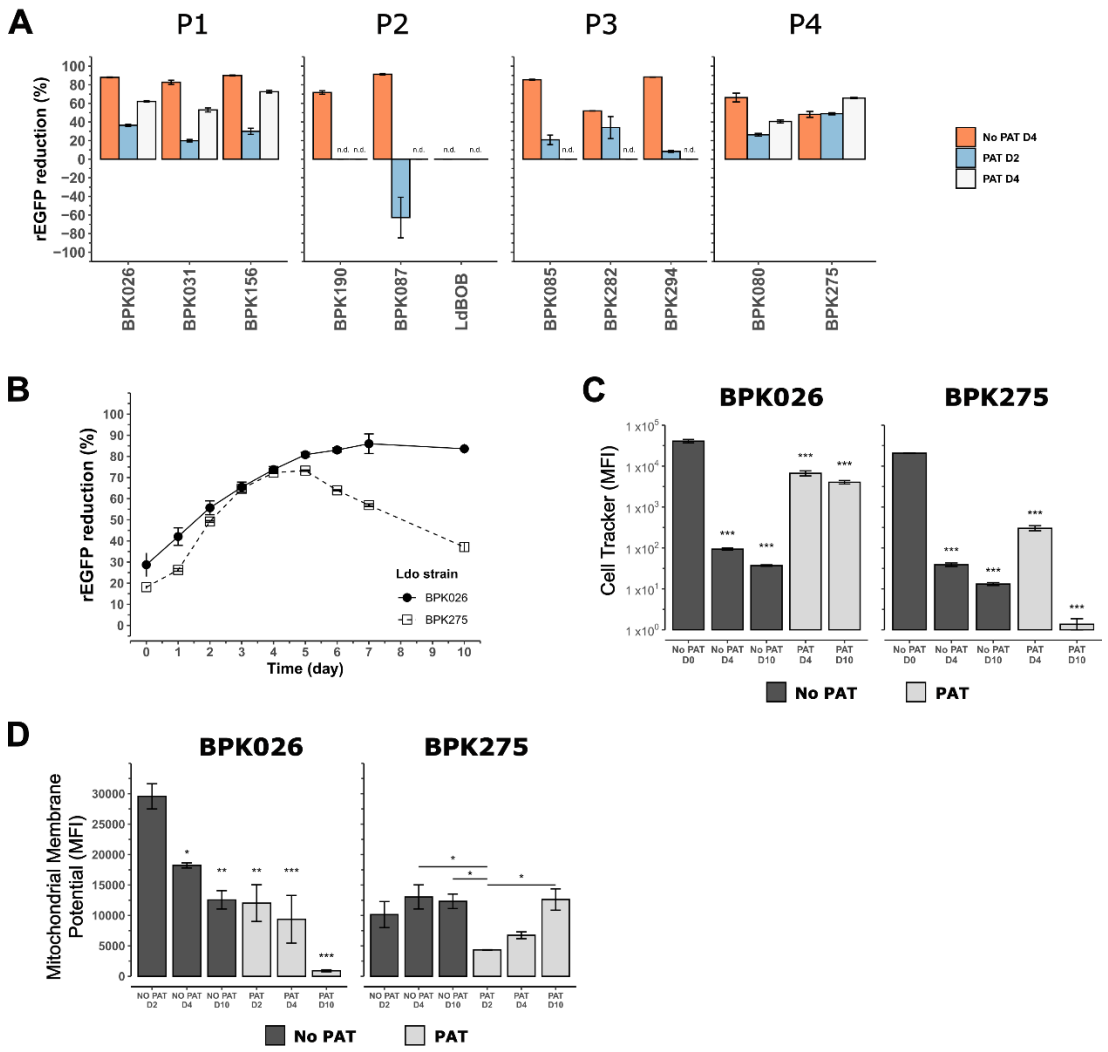

Figure 2. Quiescence features of *L. donovani* promastigotes under prolonged PAT exposure. (**A**) rEGFP expression reduction in percentage in P1-P4 profiles under normally lethal doses of PAT exposure for 2 (PAT D2) and 4 (PAT D4) days. A group without exposure for 4 days was included (No PAT D4). In certain samples, rEGFP expression data is not reported due to a limited number of viable cells, indicated as 'n.d.' (not determined). (**B**) rEGFP expression reduction in percentage in BPK026 and BPK25 from day 0 to 10. (**C**) Proliferation status measured by CellTracker in promastigotes from BPK026 and BPK275 under PAT exposure (PAT) with the respective no-drug controls (No PAT). The results were compared to the initial staining point of the parasites (No PAT D0). (**D**) Measurement of the mitochondrial membrane potential with MitoProbe ™ DilC by flow cytometry in promastigotes exposed for 2, 4, and 10 days to strain-specific PAT normally lethal dose (PAT); and the respective controls without drug (No PAT). The results were compared to promastigotes at the logarithmic state (No PAT D2). (**A,B**) The rEGFP expression reduction in percentage was calculated by comparison of the signal of each group to promastigotes without PAT exposure at the logarithmic state. The data reflects the mean ± SEM of three biological replicates. The asterisks represent the statistically significant difference after Tukey's post-hoc test; * P < 0.05, ** P < 0.01, *** P < 0.001.

<u>The impact of transition through quiescence during exposure to PAT on antimony susceptibility depends on the presence of genomic pre-adaptations to antimony in analysed *L. donovani* lines</u>

Although the quiescent state was found in all but one of the studied lines, the different killing profiles observed earlier, suggested different survival mechanisms. Specifically, P1 parasites seemed to behave similarly to classical bacterial persisters with no growth during exposure to the drug, while P3 and P4 parasites were able to resume growth under drug exposure after a short transition through the quiescent state, suggesting that a small subpopulation of these resistant parasites became hyper-resistant. To ascertain whether drug-pressure was selecting for altered genome sequences of parasites

257 isolated post-exposure to PAT, we analysed the PAT-recovered parasites with particular focus on their
258 PAT susceptibility and potential genomic alterations.

259 First, we measured the PAT susceptibility of the cells that recovered from the PAT exposure by
260 comparing the IC_{50} without drug exposure (No PAT) and after removal of PAT and recovery of growth
261 (Post-PAT) (Table 2). As reported previously, we found that the P1 parasites (ISC1 group) showed the
262 highest susceptibility, with IC_{50} values ranging between 9 ± 0.6 and 19 ± 1.2µM. The P3 and P4 parasites
263 exhibited a lower susceptibility, with IC_{50} values ranging between 46.4 ± 0.5 µM and 137.1 ± 11.9 µM.
264 When control and Post-PAT conditions were compared, two patterns were observed: (i) P1 lines did not
265 show changes in IC_{50} after the exposure to PAT; (ii) in contrast, the P3 and P4 lines showed a significant
266 increase of IC_{50} in Post-PAT conditions. The result observed for the P1 parasites is consistent with the
267 classical behaviour reported for persister cells in bacteria. However, the extreme increase in IC_{50} values
268 in such a short period of time observed for P3/P4 parasites was unexpected, but consistent with the
269 ability of these parasites to grow in the presence of PAT.

270

271 **Table 2.** Drug susceptibility of *L. donovani* promastigotes (IC_{50}, µM) of ten ISC and one reference strain measured by resazurin
272 assay after removing normally lethal dose 10-day of PAT (post-PAT); the control (No PAT) was maintained in parallel and not
273 exposed to the drug. For three lines that did not recover after drug exposure, the data is not reported and denoted as 'n.d.'
274 (not determined). The data is presented as the mean ± SEM of three biological and technical replicates.

Strain	H-locus amplified	AQP1 indel†	IC50 PAT No PAT	IC50 PAT Post-PAT
P1				
BPK026	no	no	9.0 ± 0.6	6.7 ± 0.7
BPK031	no	no	19.0 ± 1.2	20.9 ± 4.6
BPK156	no	no	18.2 ± 0.7	19.7 ± 0.1
P2				
BPK190	yes	no	nd	nd
BPK087	yes	no	nd	nd
LdBOB	no	no	nd	nd
P3				
BPK085	yes	no	89.9 ± 0.5	241.5 ± 14.7
BPK282	yes	no	137.1 ± 11.9	423.5 ± 2.8
BPK294	yes	no	40.2 ± 4.4	230.1 ± 13.9
P4				
BPK080	yes	no	52 ± 1.7	86.8 ± 2.6
BPK275	yes	yes	46.4 ± 0.5	214.1 ± 30.1

275 † Indel associated with antimonial resistance.

276

277 We then, we sequenced and compared the genome of control and Post-PAT, in triplicates, in order
278 to search for possible signatures of drug resistance. In our analysis, we focused on potential changes
279 of SNPs, INDELs, copy number of individual genes and the H-locus and somy values. Because of ISC1
280 strains/P1 parasites having much higher number of heterozygous SNPs in comparison to other strains
281 [16], we carried out the analysis of P1 and P3/4 parasites separately. In both P1 and P3/4 lines, we did
282 not observe consistent (*i.e.* present in all three replicates) SNP/indel changes (Fig. 3A,B; Supp. Fig. 5)
283 changes. Similarly, there were no consistent changes in the depth of individual coding sequences (Fig.
284 4A,B; Supp. Fig. 6), including the MRPA genes (Supp. Table 4) when No- and Post-PAT parasites were
285 compared. However, when we analyzed somy changes in Post-PAT parasites as compared to non-
286 exposed lines, we observed a general decrease of somy of several chromosomes in both P1 and P3/4

287 lines (Fig. 5; Supp. Fig. 7). Focusing on the somy changes that we consider biologically significant (S
288 values difference of at least 0.5, p-value≤0.05), we detected: i) decrease in at least one chromosome
289 in all P1 parasites, namely chr 33 and chr07 in BPK026, chr 23 in BPK031 and chr 09 in BPK156. In
290 addition, five chromosomes, chr 02, chr 08, chr 14, chr 32and chr 35 were decreased in BPK085, and
291 chr 26 in BPK294 ii) no significant increases in chromosome copy number were found in P1 parasites,
292 while we observed a significant increase in copy number of chr 6 and ch31 in BPK282 and BPK275. In
293 addition, an increase (albeit not reaching statistical significance) in chr 31 was found in BPK294, where
294 chr 07 was also increased. No significant aneuploidy changes were detected in BPK080.

295 In summary, no consistent genomic alterations could be detected in either P1 or P3/4 parasites.
296 This further supports persister-like nature of a small population in P1 parasites that survive normally
297 lethal doses of PAT. In the case of P3/P4 parasites, we report here detection of a unique form of
298 transient persisters with the ability to retain their reduced PAT susceptibility in drug-free conditions
299 showing no discernible genetic change when compared to the precursors. Further investigation,
300 possibly into epigenetic modification is required to ascertain the mechanism allowing the growth in
301 PAT and increase of IC_{50} in recovered P3/P4 parasites.

302 Overall, the impact of the transition through quiescence, on drug susceptibility differed, depending
303 on the presence of genomic pre-adaptations to antimony. Lines without any genomic pre-adaptation
304 exhibited features of a classical quiescence phenomenon linked to the presence of persisters, where
305 increased tolerance to a drug is restricted to the quiescence phase. Consistent with this notion, no clear
306 drug resistance signatures were detected in Post-PAT parasites. While in the lines that were genomically
307 pre-adapted, after a short period of quiescence, a subpopulation of more tolerant cells was able to
308 resume growth even in the presence of PAT. These emergent cells had a level of PAT resistance beyond
309 the level of the parent clone in which quiescence was initially induced. However, no consistent genomic
310 changes could be detected in the analyzed P3/P4 parasites. This suggests a presence of a unique form
311 of adaptation in these lines, in which the exact molecular mechanism underlying the reduced PAT
312 susceptibility remains to be characterized.

313

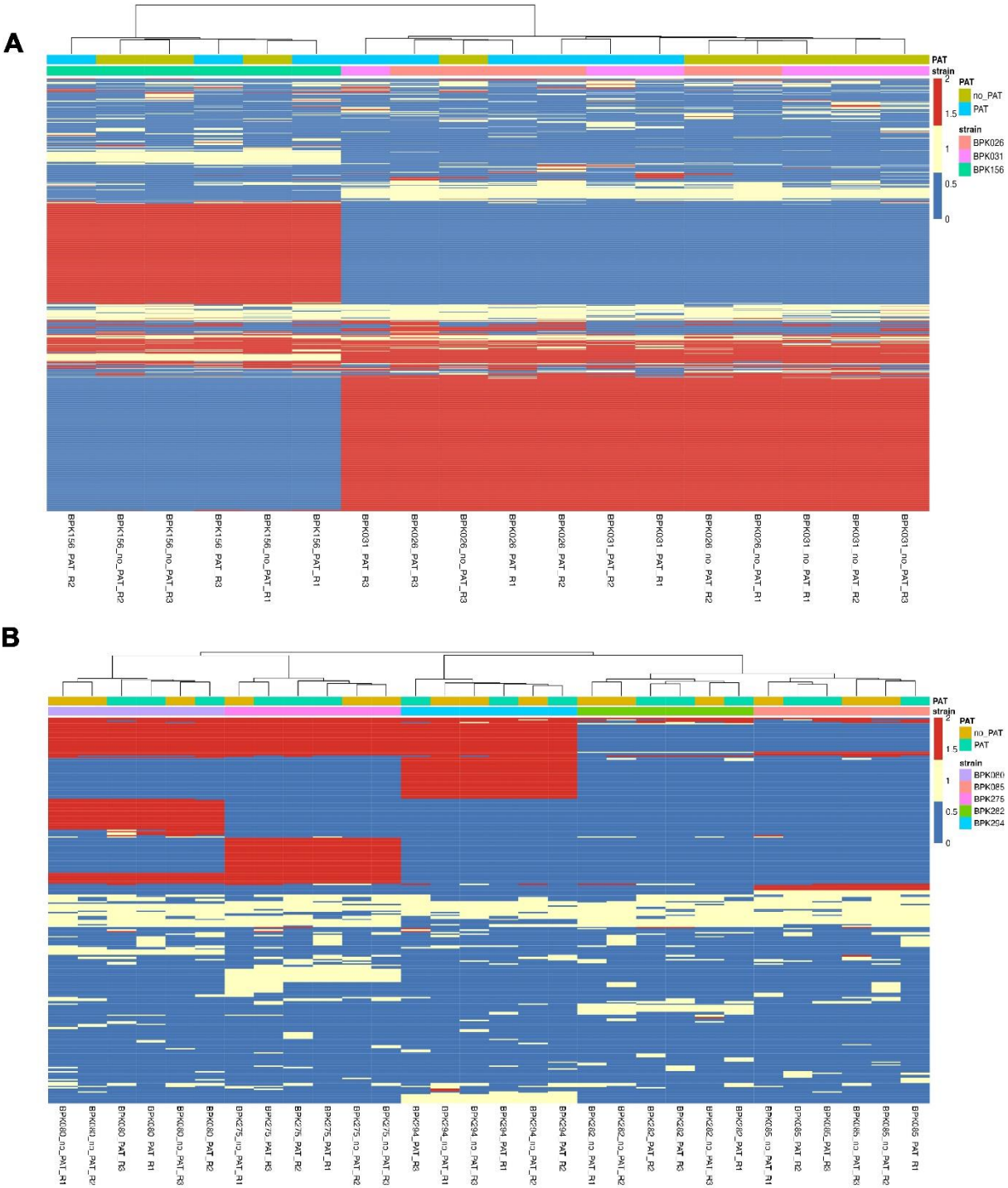

Figure 3. Heatmap illustrating the distribution of single nucleotide polymorphisms (SNPs) across strains belonging to (**A**) Profile 1 and (**B**) Profiles 3/4. SNPs that exhibited no variation across the 30 Profiles 3/4 samples or the 18 Profile 1 samples were filtered out. The color scheme categorizes SNPs as follows: blue represents the absence of a SNPs, yellow indicates heterozygous SNPs, and red denotes homozygous SNPs. Hierarchical clustering of samples (columns) and SNPs (rows) was performed using the complete linkage method with Euclidean distance. A color-coded bar above the heatmap indicates whether each strain was exposed to PAT, alongside the strain names. The data represents three biological replicates (R1, R2, R3) after removing normally lethal doses of PAT (PAT), and their respective control without drug (no_PAT).

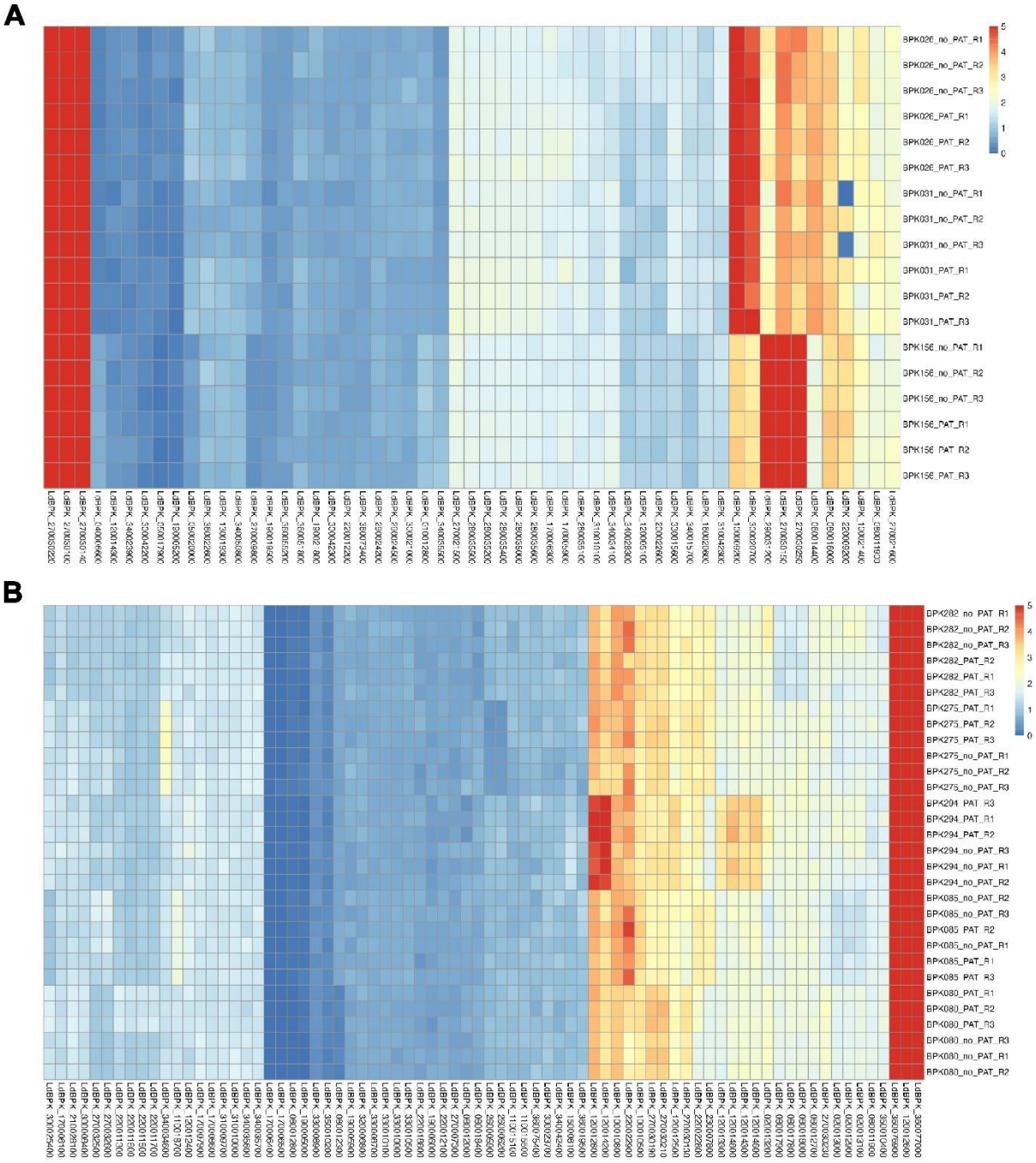

Figure 4. **Heatmap of the** (**A**) Profile 1 and (**B**) Profiles 3/4 strains, displaying CNV values for genes with a statistically significant 50% increase or decrease in CNV. Statistical significance was determined using a Student's t-test to compare CNV values between PAT-exposed (PAT), and non-exposed replicates (No_PAT) for each strain. Three biological replicates were included (R1,R2,R3) for each strain and drug exposure.

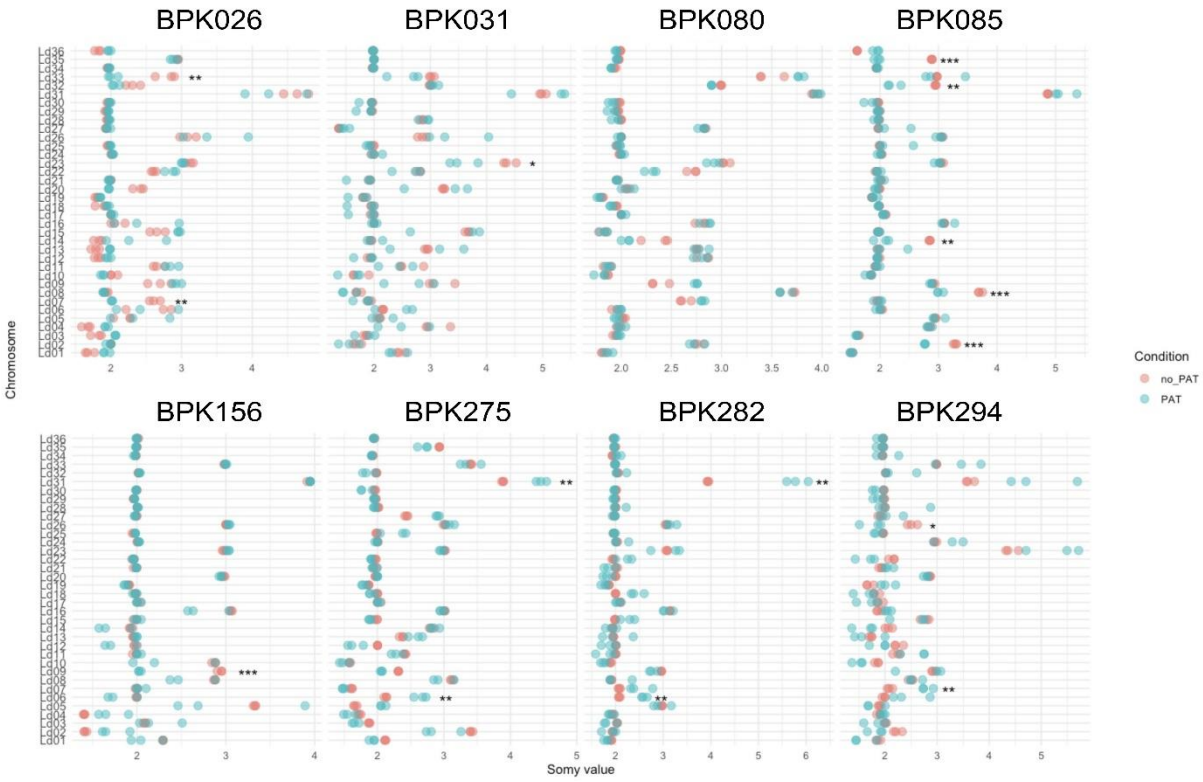

Figure 5. Dot plot containing the somy values per chromosome and per strain. For each chromosome and each strain, the somy value is indicated in the non-exposed samples (red, No_PAT) and the PAT exposed sample (green, PAT). Statistically significant somy differences using student t-test between non-exposed versus PAT-exposed samples are indicated by asterisks per chromosome and strain (* < 0.05, ** < 0.01, *** < 0.001). The data represents the values of three biological replicates.

PAT-tolerant promastigotes show cross-tolerance to other drugs

In bacteria, entering into a non-proliferative physiological state after the exposure to one drug, can provide tolerance to other antibiotics [6–8]. Hence, we tested whether the observed PAT tolerance, associated with the acquired quiescent state in the BPK026 and BPK275 lines, would also provide tolerance to other known antileishmanial compounds. We, therefore, evaluated the susceptibility of PAT-tolerant promastigotes of both BPK026 and BPK275 towards 5 compounds with different modes of action: amphotericin B (AMB), miltefosine (MIL), bortezomib (BOR), carbonycil (FCCP) and paromomycin (PARO). Briefly, i) AMB binds ergosterols and potentially destabilises membranes, ii) MIL is a lipid binding compound and likely also acts through destabilization of membranes, iii) BOR is a proteasome inhibitor, iv) FCCP is a protonophore, which can permeabilise the mitochondrial membrane, and v) PARO is a probable protein synthesis inhibitor [38–42]. First, we found that the IC_{50} values for each of these compounds were comparable in BPK026 and BPK275 (Supp. Table 5). To assess the protective effect of PAT-associated tolerance, we first triggered quiescence by exposing the promastigotes to PAT (strain-specific normally lethal doses) for 5 days, followed by 5 days of simultaneous exposure of PAT and the additional drug (serial exposure (S), Supp. Table 6). Secondly, we added both PAT and the second drug from the very beginning (combination exposure (Co), Supp. Table 6). The drugs were applied at their respective IC_{50} concentrations in both Co and S conditions. As a control exposure, we repeatedly treated with PAT during the first and second exposure (Supp. Table 6). To assess the killing effect of these drugs, we quantified the % of viable promastigotes in relation to the control exposure (C).

353 In the case of BPK026, two main patterns were observed. On one hand, with AMB, MIL, and BOR,
354 there was a strong reduction of the viability ratio in respective combination exposures (0.001 to 0.34
355 range), while in the serial exposures, the viability was comparable to the levels in control treatment
356 (0.79-0.82 values in S, and 1.0 in C; Fig. 6A). This indicates that PAT-triggered BPK026 quiescent cells
357 gain tolerance to AMB, MIL, and BOR. On the other hand, with FCCP and PARO, viability remained
358 similar to control exposure in both Co and S conditions, suggesting that used concentrations of FCPP
359 and PARO were too low to enhance PAT killing (Fig. 6A). Results were confirmed by the reversibility
360 assay: *i.e.* the combination of PAT+AMB for which growth was observed in only one out of three
361 replicates, while all three replicates demonstrated proliferation in the case of serial exposure (Table 3).
362 In the case of BPK275, results were different and 5 patterns were observed (Fig. 6A): (i) for BOR, a low
363 viability ratio in Co (0.047 ± 0.02 value), and comparable viability in the C exposure and S exposures,
364 suggesting cross-tolerance to BOR in PAT-exposed quiescent cells, ii) lower viability ratios for AMB (both
365 Co and S exposures) in comparison to C, but the viability in S was significantly higher than in Co,
366 suggesting some level of protection against AMB provided by quiescence of PAT-exposed cells (iii) same
367 viability as control for MIL (both Co and S conditions), indicating that used MIL concentrations were too
368 low to enhance PAT killing, (iv) for FCCP, although low viability in S was observed, microscopic
369 examination revealed an abundance of parasites, suggesting that parasites likely died due to nutrient
370 deprivation, and (v) for PARO a higher viability ratio in Co exposure in comparison to C and a ratio close
371 to the control under serial exposure, suggesting that PARO and PAT act synergistically to trigger the
372 presence of quiescent cells. In all conditions, the reversibility assay revealed proliferation in the 3
373 replicates (Table 3). Collectively, these results show that PAT-tolerant cells also show tolerance to other
374 drugs, but the degree of this cross-tolerance is drug- and strain-dependent.

375 To analyze the cross-tolerance further we focused on protection against BOR, for which we also
376 executed combination and serial exposure and compared the effects of applying BOR at 3 different
377 concentrations: at 1x, 2x, and 5x IC_{50} of BOR (see experimental design in Supp. Table 7). In the case of
378 BPK026, viability ratios slightly decreased with the increasing concentration of BOR in the combination,
379 condition, but this did not affect the observed cross-tolerance in S exposure (Fig. 6B). In contrast, in
380 BPK275, viability ratios decreased with the increase of BOR concentration in both conditions, with
381 almost no viable cells detected in the two highest concentrations of BOR. (Fig. 6B). The reversibility
382 assays showed that none of the Co replicates could grow, while a few replicates in the S condition could
383 re-proliferate in BPK026. By contrast, for BPK275, all replicates in the S condition could reactivate, while
384 only two or none were able to proliferate in the higher concentrations of BOR in Co exposure (Table 3).
385 This indicates that cross-tolerance to BOR could be observed for both strains, but it was more
386 pronounced for the antimony resistant BPK275 line.

387

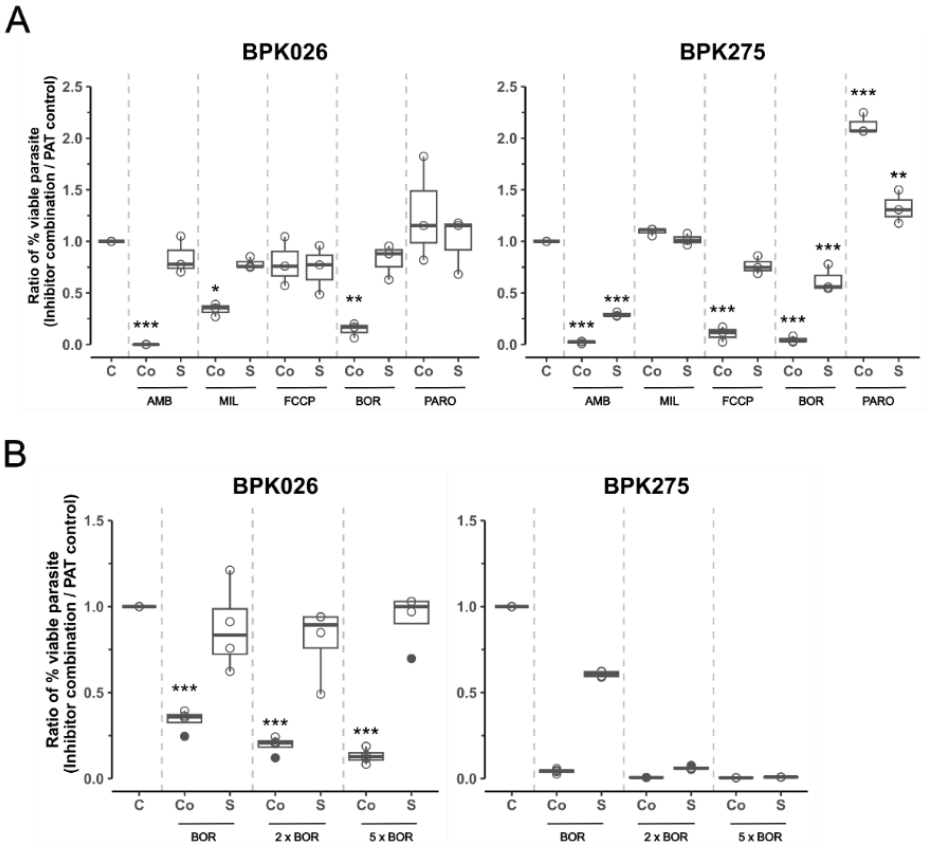

Figure 6. Survival of PAT-tolerant *Leishmania* promastigotes when exposed to other drugs. (**A**) Ratio of percentages of viable parasites submitted to different compounds (IC50) vs normally lethal doses of PAT (control, C) and following two drugging schemes (Co, combination and S, serial); (i) MIL, Miltefosine; AmB, Amphotericin B, PARO, Paromomycin; BOR, Bortezomib and FCCP, Carbonycil. Plotted data shows the mean ± SEM of three biological replicates for each combination or serial. (**B**) Ratio of percentages of viable parasites submitted to BOR (1x IC50, 2x and 5x IC50) vs normally lethal doses of PAT (control, C) and following two drugging schemes (Co and S). Plotted data shows the mean ± SEM of four biological replicates for each combination or serial. The asterisks indicate statistically significant differences for each scheme compared to the control, analyzed by Tukey's post-hoc test (**A**) and Student's t-test, (**B**)* $P < 0.05$, ** $P < 0.01$, *** $P < 0.001$.

Table 3. Reactivation of parasite proliferation (numbers out of 3 or 4 replicates) after exposure to a combination of PAT and another drug or serial drugging (see experimental design in Supp. Table 6 or Supp Table 7).

Condition	Drug/Inhibitor	P1	P4	Drug/Inhibitor	P1	P4
		BPK026	BPK275		BPK026	BPK275
Control	PAT	3 of 3	3 of 3	PAT	4 of 4	4 of 4
Combination	AMB	1 of 3	3 of 3	BOR	0 of 4	4 of 4
Serial		3 of 3	3 of 3		0 of 4	4 of 4
Combination	MIL	3 of 3	3 of 3	2 x BOR	0 of 4	2 of 4
Serial		3 of 3	3 of 3		1 of 4	4 of 4
Combination	FCCP	2 of 3	3 of 3	5 x BOR	0 of 4	0 of 4
Serial		1 of 3	3 of 3		1 of 4	4 of 4
Combination	BOR	0 of 3	3 of 3			
Serial		1 of 3	3 of 3			
Combination	PARO	3 of 3	3 of 3			
Serial		3 of 3	3 of 3			

400 **Discussion**

401 This study demonstrates that genetically different *L. donovani* strains use quiescence as a survival
402 strategy under normally lethal doses of trivalent antimony. In most lines, upon exposure to PAT a small
403 non-replicating population with reduced metabolism was observed and had the ability to survive the
404 treatment. A quiescence state was also found in an antimony resistant *Leishmania* line, in which a
405 majority of cells survived drug exposure. Quiescence was detected in all parasites with genomic pre-
406 adaptation to antimony, and these cells could also resume growth while still under treatment exposure,
407 enhancing the level of resistance to PAT in so doing. Quiescence, therefore, appears to be a widespread
408 phenomenon in *Leishmania* parasites exposed to normally lethal doses of a drug.

409 Here we triggered entry into quiescence by exposure to antimony, analogous to triggered
410 persistence in bacteria rather than spontaneous persistence [4]. All lines surviving normally lethal doses
411 of PAT, showed a bi-phasic time-kill curves typical for bacterial persister cells [43,44], though in two lines,
412 BPK275 and BPK080, the subpopulation of PAT tolerant cells was larger than typical. Detailed analysis
413 of the lines with the most extreme survival phenotypes revealed several properties typical of persisters,
414 including reduction of metabolism, proliferation and mitochondrial membrane potential with no
415 apparent genomic changes and cross-tolerance to other antileishmanial drugs. However, the ability to
416 resume growth after a transient adoption of quiescence observed in lines with pre-existing antimony
417 resistance is inconsistent with classical definition of bacterial persisters, since these lines acquire a
418 further reduction in sensitivity to drug during the passage through quiescence. Because of this unique
419 mixture of observed phenotypes in the quiescent *L. donovani* lines, we collectively call them persister-
420 like cells.

421 Parasites without known antimony resistance, when triggered to enter quiescence over a 10-day
422 period remain quiescent while still under drug treatment, and resume growth only when transferred
423 to antimony-free medium. By contrast, *Leishmania* that had harboured genetic mutations that yielded
424 resistance to antimony, also entered quiescence when exposed to antinomy at a dose beyond that to
425 which they are normally resistant. However, these cells were able to re-enter growth phase whilst in
426 medium containing drug. Remarkably, these parasites that resume growth whilst still in medium
427 containing antimony are actually more resistant to the drug than they were before having passed
428 through quiescence. Although we do not have a molecular explanation for this, it is possible that the
429 MRPA pump which removes antimony from the cells [45], and is amplified as part of the H-locus in
430 resistant cells is expressed at still higher levels independently of gene copy number (which was not
431 further amplified during the quiescence period). Given that drug-efflux is a common mechanism of
432 resistance in these strains, it is possible that the resistant lines reach a point at which the intracellular
433 levels of antimony decrease below a threshold required to retain the triggered quiescence phenotype.
434 It will be interesting to explore this in future work.

435 We also tested the ability of cells in which quiescence was triggered by PAT to tolerate exposure to
436 a range of other drugs. By adding 5 other compounds, with different modes of action, at their IC_{50}
437 levels, alongside PAT on day zero, we were assessing their toxic effect on non-quiescent cells. By
438 contrast, by adding the secondary drugs five days after the addition of PAT, we were testing their ability
439 to kill pre-selected quiescent cells. AMB, MIL and BOR had significantly reduced ability to clear cultures
440 if added after 5 days while this was not the case for PARO and FCCP. Mechanistically we had assumed
441 AMB might not have different impact on quiescent cells as it permeabilised membranes after binding
442 ergosterol. However, quiescent cells appear to be less sensitive to the drug, possibly indicating

443 membrane remodelling during quiescence, which might also explain why quiescent cells also showed
444 tolerance to MIL. In the case of the proteasome inhibitor BOR, the general decrease in protein turnover
445 in quiescent cells may explain why cross-tolerance is seen to this compound. FCCP interferes with
446 proton-dependent transport processes at the mitochondrial and plasma membranes and given the
447 requirement to sustain key metabolic processes the fact that quiescent cells retain sensitivity was not
448 a surprise. As an inhibitor of protein synthesis paromomycin likely continues to act on processes crucial
449 to the viability of quiescent cells, which would explain the absence of cross-tolerance to this drug.

450 Cross-tolerance to several antifungal compounds has been observed in pathogenic fungi and was
451 linked to changes in aneuploidy patterns and not the persister state [46,47]. Interestingly, it has been
452 reported by us and others that aneuploidy is very dynamic and can be adaptive in *Leishmania* [19,32,33,48,49]
453 . We analyzed genomic changes in both lines that showed cross-tolerance, but only in the recovered
454 parasites grown in drug-free medium, where no consistent chromosome copy number variations were
455 found. However, given the aneuploidy dynamics and mosaicism in *Leishmania* we cannot exclude that
456 some chromosome copy number changes contributed to the detected cross-tolerance in persister-like
457 cells.

458 In our experimental set up, the impact of transition through quiescence extends beyond the
459 duration of the non-proliferative period. We found that the lines with pre-existing adaptations to
460 antimonials (through amplification of a drug exporter and/or inactivation of AQP1 transporter)
461 emerged with reduced PAT susceptibility after recovering growth in drug-free condition. Given the lack
462 of detected genetic changes in those parasites, and the isogenic nature of the used lines we propose
463 that a form of resetting mechanism takes place, perhaps through epigenetic reprogramming that
464 explains this phenomenon. Consistent with that, Dirkx and colleagues reported previously that
465 transition through quiescence increases the parasite's infectivity and transmission potential [26].

466 The 11 *L. donovani* lines studied here exhibited here a range of quiescence and persister
467 phenotypes, which may be exploited further to probe the molecular mechanism that control the
468 transition to, maintenance and exit from quiescent state. For example, BPK087 did not exhibit
469 reduction of rEGFP expression in the very early timepoints of exposure, resulting in rapid killing. This
470 suggest that this line was not able to enter quiescence in our experimental conditions. It would be
471 interesting to see whether this remains the same if different doses of PAT are applied. If BPK087 proves
472 to be unable to enter into quiescence in response to PAT pressure, it could serve as a useful model to
473 uncover signalling that leads to quiescence entry. At the same time, several lines characterized by
474 profile 3 exhibited the ability to exit quiescence still under drug pressure and could be employed to
475 uncover the mechanisms controlling the maintenance and promoting the exit of quiescent state.

476 This study was carried out with the extracellular promastigote form of *Leishmania* and should be
477 repeated with both axenic and intracellular amastigote forms to confirm the same phenomena are
478 applicable to the clinically relevant stage. Several studies have already indicated the existence of
479 persister-like cell in *Leishmania* infections of mammals and it seems increasingly likely that *L. donovani*
480 persister-like cells can explain some cases of treatment failure in the absence of drug resistance and
481 post-kala azar dermal leishmaniasis (PKDL), observed years after clinical healing of VL.

482 In summary, this report demonstrates a worrying, intrinsic ability of *Leishmania* to tolerate high
483 lethal doses of a drug and exhibit cross-tolerance to different drugs, even with non-overlapping modes
484 of action. We also unravel unexpected effects of adoption of quiescence, which may go beyond the

485 period of exposure to drug. In strains with pre-existing genomic adaptations to the drug, transition
486 thorough the quiescent state potentially facilitates the development of a form of population-wide
487 super drug resistance. Thus, even a short period of quiescence may have much more serious impact
488 than previously thought, with a potential to create super-resistant parasites.

489

490 **Methods**

491 **Parasites**

492 Eleven strains of *L. donovani* were used in this study (Table 01). Ten were derived from clinical
493 isolates originating from VL patients in Nepal and classed into 3 main genotypes according to the
494 amplification or not of H-locus (containing MRPA) and AQP1 sequence [16] (i) No amplification of H-locus
495 and wild type AQP1 (H-/AQP+): MHOM/NP/2002/BPK026/0 clone 5 (LdBPK026),
496 MHOM/NP/2002/BPK031/0 clone 2 (LdBPK031) and MHOM/NP/2002/BPK156/0 (LdBPK156). **(ii)**
497 Amplification of H-locus and wild type AQP1 (H+/AQP+): MHOM/NP/2002/BPK080/0 clone 1
498 (LdBPK080), MHOM/NP/2002/BPK085/0 clone 8 (LdBPK085), MHOM/NP/2002/BPK087/0 clone 11
499 (LdBPK087), MHOM/NP/--/BPK190/0 clone 3 (LdBPK190), MHOM/NP/2003/BPK282/0 clone 4
500 (LdBPK282), MHOM/NP/2003/BPK294 clone 1 (LdBPK294). **(iii)** Amplification of H-locus and AQP1 indel
501 in position Ld31_0007735 (H+/AQP-): MHOM/NP/2003/BPK275/0 clone 18 (LdBPK275). A last strain
502 originating from Sudan was used as a reference: MHOM/Sudan/1962/1S-2D Bob (LdBOB). All strains
503 were cryopreserved at the Institute of Tropical Medicine in Antwerp, Belgium. Promastigotes were
504 maintained at 26°C in M199 medium (Thermo Fisher) at pH 7.2 supplemented with 20% of heat-
505 inactivated fetal bovine serum (HI-FBS), 5 mg/mL hemin, 10µM acid folic, 1X RPMI vitamin mix, 2mM
506 glutamine, 100 units/mL of penicillin, and 100 µg/mL of streptomycin, which was referred to as M199-
507 sup in the following experiments. For transfections, HOMEM medium (Gibco) supplemented with 20%
508 HI-FBS, referred to as HOMEM-sup, was used to transfect *Leishmania* promastigotes mentioned below.

509 **Drugs**

510 The drugs used in this study were: i) for leishmaniosis treatment: potassium antimonyl tartrate,
511 (383376, Sigma-Aldrich), miltefosine (M5571, Sigma-Aldrich), amphotericin B (A2942, Sigma-Aldrich),
512 and paromomycin (P5057, Sigma-Aldrich); ii) in development: bortezomib (5.04314, Sigma-Aldrich),
513 and carbonyl cyanide 4-(trifluoromethoxy) phenylhydrazone (C2920, Sigma-Aldrich). The stock
514 solutions of potassium antimonyl tartrate (PAT), paromomycin (PARO), and miltefosine (MIL) were
515 dissolved in PBS, meanwhile bortezomib (BOR), and carbonyl cyanide 4-(trifluoromethoxy)
516 phenylhydrazone (FCCP) in dimethylsulfoxide (DMSO) at a concentration of 20-50 mM and stored at -
517 20°C. The working solutions were freshly diluted in PBS or dimethylsulfoxide (DMSO) and added to
518 M199-sup until reaching the desired final concentrations for the different drugs/inhibitors. A control
519 containing either PBS (0.5% v/v) or DMSO (0.1% v/v), depending on which was used to dissolve the
520 drug or inhibitor, was included in the plate. The addition of PBS or DMSO did not interfere with the
521 parasite growth.

522 **Engineering of fluorescent lines**

523 For each strain, the enhanced green fluorescent protein (EGFP) was integrated within the 18S
524 ribosomal DNA locus (rEGFP) of promastigotes, with pLEXSY-hyg system (Jena Bioscience). rEGFP was
525 previously validated as a negative marker for quiescence: highly expressed in proliferative cells and
526 downregulated during quiescence [36]. For transfection, *L. donovani* promastigotes were maintained at
527 26°C in HOMEM-sup with passages each 4-7 days at a dilution 1/50. A quantity of 2 x 10^7 promastigotes
528 was transfected with 100 ng of the linearized DNA fragment containing EGFP, using the Basic Parasite
529 Nucleofector kit 1 (VMI 1011, Lonza); program U-033. After 24 hours of transfection, promastigotes
530 harboring rEGFP were selected with hygromycin B at a final 25 µg/ml concentration. Parasites were
531 passaged 3 times in HOMEM-sup with hygromycin B until the isolation of individual clones. An

532 appropriate dilution of 2-day promastigotes culture was washed with PBS and adjusted to a
533 concentration of 2 x 10^6 parasites/mL in PBS containing 2% HI-FBS, 100 units/mL of penicillin, and 100
534 µg/mL of streptomycin. Then, the suspension was filtered using a 5-µM pore filter to remove cell
535 clumps. A total of 8 individual clones were sorted by fluorescence-activated cell sorting (FACS), using
536 S3e TM Cell Sorter (BIORAD) using a 488 nm laser for EGFP excitation. Single cells expressing EGFP were
537 selected based on FSC-A vs SSC-A followed by FSC-A vs FSC-H, and FSC-A vs EGFP, and collected into
538 300 µL of HOMEM-sup. The clonal expansion was monitored for two weeks until enough promastigotes
539 were present for further passages. The EGFP fluorescence of the clones was assessed by FACSVerse
540 cytometer (BD Biosciences), where the clones with more than 99% of cells expressing EGFP and the
541 highest median fluorescence intensity (MFI) were selected for further experiments. The generated lines
542 were called rEGFP lines, maintained in M199-sup, and then cryo-preserved.

543 **Estimation of PAT concentration at which parasites reach a minimal metabolic activity**

544 Promastigotes of the *L. donovani* rEGFP lines were synchronized by consecutive passages every two
545 days to ensure that the promastigotes were in the proliferative phase. Then, parasites were distributed
546 (5x10^5 parasites/mL) in 200µL of M199-sup in sterile 96-well culture plates and exposed to different
547 concentrations of PAT ranging from 1200 to 12.5 µM for 4 days at 26°C. An additional well was included
548 with only M199-sup as a control for each *L. donovani* line. Resazurin sodium salt (Sigma) was added at
549 a final concentration of 80µM, and incubated for 5 h in the dark at 26°C. The fluorescence was
550 measured using the Victor X2 Multilaber Reader (PerkinElmer) with a 560 excitation and 590 emission
551 wavelength. The fluorescence measurements for each line were normalized in comparison to their
552 respective control with only M199-sup to calculate the percentage of cells with metabolic activity. The
553 lethal PAT concentrations for each line were determined as the drug concentration point where the
554 percentage of metabolic active cells was less ~1%.

555 **Monitoring quiescence and cell viability during PAT exposure**

556 The rEGFP lines were passaged twice each two days to synchronize them at the logarithmic phase
557 and then a density of 5x10^5 parasites/ml was exposed to a normally lethal PAT doses during 10 days at
558 26°C where M199-sup with PAT was refreshed once after 5 days. The respective controls were prepared
559 for each line with only M199-sup, and promastigotes were collected daily. At each time point, parasites
560 were centrifugated at 1800 x g for 10 minutes, resuspended in PBS with 1 µM NucRed Dead 647
561 (Thermo Fisher), a dead marker that binds to DNA when the cell membrane is damaged and emits
562 fluorescence. After 10 minutes at room temperature, the samples were analyzed by FACSVerse (BD
563 Biosciences) cytometer including as controls: (i) negative control, wild-type line, and not-stained, and
564 (ii) a dead control, parasites exposed to thermal shock at 70°C for 10 minutes. The gating scheme was
565 initiated with a large gate of FSC-A vs SSC-A to include all cells due to the heterogeneous size and
566 complexity of the parasites, continued with FSC-H vs FSC-A gate to avoid doublets or aggregates. A gate
567 of FSC-A vs NucRed Dead (-) was used to exclude dead cells, and live cells were determined based on a
568 gate of NucRed Dead (-) vs EGFP(+). The Flow Cytometry Standard (FCS) data files were analyzed with
569 the FlowJo™ v10.10 to determine the median fluorescence intensity (MFI) of EGFP and the percentage
570 of viable cells.

571 **Reversibility test**

572 Promastigotes from the different *L. donovani* rEGFP lines under PAT exposure during all the
573 combination and serial conditions were harvested and washed once with M199 medium by

574 centrifugation at 1800 x g for 10 minutes. The supernatant was removed without disturbing the pellet,
575 resuspended in M199-sup, and incubated at 26°C. Then, we monitored the cultures weekly for 21 days
576 under microscopic observation until flagellated mobile promastigotes were observed.

577

578 **Promastigote susceptibility assay**

579 Susceptibility of the promastigotes was assessed in the eight lines that survive PAT exposure and
580 revert to a proliferative state, including their respective controls maintained in only M199-sup medium.
581 Likewise, the promastigotes of BPK026 and BPK275 were used to measure the susceptibility against
582 five drugs for the cross-tolerance experiments. The measurement was performed using the resazurin
583 method as previously described with minor modifications [20,50]. Briefly, logarithmic-stage promastigotes
584 ($5x10^5$ parasites/mL) were plated in 200µL of M199-sup in sterile 96-well culture plates and grown in
585 the presence of M199-sup alone (control) and medium containing serial dilution of drugs for a period
586 of 72 h at 26°C. Then resazurin sodium salt (Sigma) was added at a final concentration of 80 µM, and
587 the parasites were incubated for 5 h at 26°C protected from light. The fluorescence was recorded with
588 an excitation/emission 560/590 nm using the Victor X2 Multilabel Reader (PerkinElmer). All
589 experiments were done with three independent cultures with two or three technical replicates each.
590 The IC_{50} (50% inhibitory concentration measurement) was calculated with GraphPad Prism 8 using a
591 sigmoidal dose-response model with variable slope.

592 **DNA preparation and bulk whole-genome sequencing (WGS) analysis**

593 Promastigotes were harvested from the eight lines that reverted to a proliferative state after PAT
594 exposure or controls maintained without it. The parasites were washed with PBS and the genomic DNA
595 was extracted using the QIAamp DNA Mini Kit (51306, Qiagen) following the manufacturer's
596 recommendations. The DNA concentration was measured using the Qubit dsDNA Quantification Assay
597 Kit broad-range (Q32853, Thermo Fisher). The libraries PCR-free were prepared and sequenced on the
598 Illumina NovaSeq6000 platform using 2 x 150 bp paired-end reads aiming for a sequence depth of
599 ~100x for each sample, a service provided by GenomeScan (Netherlands).

600 After quality control of the raw fastq files using FastQC, the reads were mapped to the *L. donovani*
601 reference genome LdBPK282-V2 [19], using BWA v0.7.17 using a seed length of 50. Reads with a mapping
602 quality higher than 30 were selected using SAMtools, duplicate reads removed using the Picard
603 MarkDuplicates command (version 2.22.4), and only properly paired reads were retained using
604 samtools. The somy values were estimated as the median reads count per million (CPM) per 10kb bin
605 of chromosomes normalized by the median CPM per bin of 5 chromosomes surrounding on both sides.
606 SNP calling was conducted using the Genome Analysis Toolkit (GATK) pipeline (version 4.1.4.1)
607 following GATK's best practices guidelines. The process included: (1) generating GVCF-formatted files
608 using GATK HaplotypeCaller, (2) combining the GVCF files from all samples with the GATK CombineGVCF
609 command, (3) performing genotyping with the GATK GenotypeGVCF command, and (4) filtering SNPs
610 and indels based on GATK's recommended best practices using the SelectVariants and VariantFiltration
611 commands. For the CNV detection, for every sample the sequencing depth per position was derived
612 using the SAMtools depth command. The CNV value was calculated by taking the ration of the median
613 coverage per gene over the median coverage of the chromosome the gene is located on. Statistical
614 tests comparing either CNV or Somy values were performed using a student's t-test. Visualization of
615 somy values, SNP data and CNV values was performed in R (version 4.2.0) using heatmaps and dot

616 plots. Heatmaps were created with the pheatmap package (version 1.0.12), while dot plots were
617 generated using the ggplot2 package (version 3.4.1).

618

619 **Determination of mitochondrial membrane potential (MMP)**

620 The BPK026 and BPK275 promastigotes were synchronized by two-day passaging in M199-sup
621 before each experiment. Several cultures were prepared with a density of $5x10^5$ parasites/mL with
622 normally lethal doses of PAT (50 µM for BPK026 and 200 µM for BPK275) at different times to have
623 samples under drug exposure for 2, 4, and 10 days with their respective controls with only M199-sup.
624 The mitochondrial membrane potential was determined using the MitoProbe™ $DilC_1$ (5) Assay Kit
625 (M341151, Thermo Fisher) based on the manufacturer's instructions. Parasites under PAT exposure
626 were centrifuged at 1800 x g for 10 minutes, the pellet was resuspended in M199 medium and
627 disaggregated into a single-cell suspension passing 6 times through a 26-G needle and syringe.
628 Promastigotes were centrifuged at 1800 x g for 10 minutes, washed once in PBS, and resuspended at a
629 concentration of $2 x10^6$ parasites/ml in PBS containing 100nM MitProbe $DilC_1$(5) for 45 minutes at 26°C.
630 Then, 1 µM SYTOX Blue Dead Cell stain (S34857, Thermo Fisher) was added to label dead cells for 5
631 minutes. In the experiment three controls were used: (i) a dead control, heat-killed parasites at 70°C
632 for 10 min, (ii) a positive control, parasites treated for 10 minutes with 200µM carbonyl cyanide m-
633 clorophenylhydrazone (CCCP) which disrupts mitochondrial membrane potential, and (iii) a negative
634 control, consisting of unstained parasites of a line without EGFP gene inserted. Also, fluorescence
635 minus one (FMO) controls were used to assess autofluorescence and establish the gates for the
636 selection of the cell populations. Subsequently, the samples were analyzed by FACSVerse cytometer
637 (BD Biosciences) using lasers 405nm for SYTOX Blue dye, 480nm for EGFP, and 640nm for MitoProbe
638 dye. Flow cytometric analysis was performed using FlowJo™ version 10.10.

639 **Proliferation analysis**

640 Approximately 1.5 x 10^7 promastigotes from *L. donovani* BPK026 and BPK275 were labeled with
641 CellTracker Deep Red (C34565, Thermo Fisher technologies) following the manufacturer's instructions.
642 Briefly, parasites were collected, washed once with PBS, and resuspended in 1 mL of M199 medium
643 containing 5 µM of CellTracker Deep Red. After 40 minutes of incubation at 26°C, cells were washed
644 with M199 medium, centrifuged at 1500 x g for 10 minutes, and resuspended in pre-warmed M199-
645 sup. Following labeling, 5 x 10^5 promastigotes/mL were treated with PAT at 50 µM (BPK026) and 200
646 µM (BPK275) in M199-sup or only M199-sup as a control and incubated at 26°C protected from the
647 light. The parasites were collected at three time points: 0, 4, and 10 days. At each measurement point,
648 promastigotes under PAT exposure were disaggregated using a 26-G needle and syringe and
649 centrifuged at 1800 x g for 10 minutes. The pellet and promastigotes from the controls were
650 resuspended in PBS at a concentration of 2 x 10^6 parasites/mL, and labeled with 1 µM SYTOX Blue Dead
651 Cell stain (S34857, Thermo Fisher) for 5 minutes in the dark, as a cell death marker. The fluorescence
652 data was acquired by FACSVerse cytometer (BD Biosciences) using lasers 405nm for SYTOX Blue dye,
653 480nm for EGFP, and 640nm for CellTracker Deep Red dye. Flow cytometric analysis was performed
654 using FlowJo™ version 10.10.

655 **Cross-tolerance experiment**

656 To evaluate tolerance to other anti-leishmanial drugs and drugs in development, of PAT-tolerant
657 promastigotes, we exposed the promastigotes of BPK026 and BPK275 to 5 drugs with different

658 mechanisms of action. We performed susceptibility tests by resazurin assay, mentioned above, to
659 calculate the IC50 estimates. As the promastigotes were already under high stress using normally lethal
660 PAT doses (50µM for BPK026 and 200µM for BPK275), we decided to use the IC50 estimates of each
661 drug. We designed an experimental design consisting of two exposure times of 5 days each, for a total
662 duration of 10 days where we had two conditions for each drug: (i) Combination, where the lethal
663 concentration of PAT and the drug (IC50 estimate) were present in both exposure times, (ii) Serial,
664 promastigotes were under normally lethal PAT concentration for the first exposure, followed by a mix
665 of PAT with the other drug for the second exposure. As a control group, promastigotes were under only
666 lethal PAT concentrations for both exposure times. The promastigotes were collected, centrifuged at
667 1800 x g for 10 minutes, and resuspended in M199 medium. The samples with large aggregates were
668 passed through 26-G to have single-cell suspension. The parasites were centrifuged again and
669 resuspended in PBS with NucRed Dead as a viability marker. The acquisition of the fluorescence data
670 and its gating scheme for analysis was the same as mentioned above.

671 **Statistical analyses**

672 Statistical analysis and data visualization were performed in R studio (R version 4.3.1) using
673 Student's t-test, with p-value < 0.05 considered statistically significant, and ANOVA followed by a post
674 hoc Tukey's multiple comparison test.

Acknowledgments

This study received financial support from the Flemish Fund for Scientific Research grant G075121N. Isolation and characterization of clinical isolates was financed by the European Commission through Leishnatdrug-R project, grant ICA4-CT-2001-10076. M.A.D. acknowledges support from Flemish Ministry of Science and Innovation.

Competing interests

The authors declare no competing interests.

Additional information

Supplementary material is available in Aroni-Soto_supplement.pdf

References

1. WHO. Antimicrobial resistance. https://www.who.int/news-room/fact-sheets/detail/antimicrobial-resistance (2023).
2. Gow, N. A. R. *et al.* The importance of antimicrobial resistance in medical mycology. *Nature Communications 2022 13:1* **13**, 1–12 (2022).
3. Darby, E. M. *et al.* Molecular mechanisms of antibiotic resistance revisited. *Nature Reviews Microbiology 2022 21:5* **21**, 280–295 (2022).
4. Balaban, N. Q. *et al.* Definitions and guidelines for research on antibiotic persistence. *Nature Reviews Microbiology 2019 17:7* **17**, 441–448 (2019).
5. Dewachter, L., Fauvart, M. & Michiels, J. Bacterial Heterogeneity and Antibiotic Survival: Understanding and Combatting Persistence and Heteroresistance. *Mol Cell* **76**, 255–267 (2019).
6. Peyrusson, F. *et al.* Intracellular Staphylococcus aureus persisters upon antibiotic exposure. *Nature Communications 2020 11:1* **11**, 1–14 (2020).
7. Nguyen, D. *et al.* Active starvation responses mediate antibiotic tolerance in biofilms and nutrient-limited bacteria. *Science (1979)* **334**, 982–986 (2011).
8. Keren, I., Shah, D., Spoering, A., Kaldalu, N. & Lewis, K. Specialized persister cells and the mechanism of multidrug tolerance in Escherichia coli. *J Bacteriol* **186**, 8172–8180 (2004).
9. Rittershaus, E. S. C., Baek, S. H. & Sassetti, C. M. The Normalcy of Dormancy: Common Themes in Microbial Quiescence. *Cell Host Microbe* **13**, 643–651 (2013).
10. Sun, S. & Gresham, D. Cellular quiescence in budding yeast. *Yeast* **38**, 12–29 (2021).
11. Amato, S. M. *et al.* The role of metabolism in bacterial persistence. *Front Microbiol* **5**, 79557 (2014).

710 12. Ponte-Sucre, A. *et al.* Drug resistance and treatment failure in leishmaniasis: A 21st century
711 challenge. *PLoS Negl Trop Dis* **11**, e0006052 (2017).

712 13. Hefnawy, A., Berg, M., Dujardin, J. C. & De Muylder, G. Exploiting Knowledge on Leishmania
713 Drug Resistance to Support the Quest for New Drugs. *Trends Parasitol* **33**, 162–174 (2017).

714 14. Mandal, S., Maharjan, M., Singh, S., Chatterjee, M. & Madhubala, R. Assessing
715 aquaglyceroporin gene status and expression profile in antimony-susceptible and -resistant
716 clinical isolates of Leishmania donovani from India. *Journal of Antimicrobial Chemotherapy* **65**,
717 496–507 (2010).

718 15. Potvin, J. E., Leprohon, P., Queffeulou, M., Sundar, S. & Ouellette, M. Mutations in an
719 Aquaglyceroporin as a Proven Marker of Antimony Clinical Resistance in the Parasite
720 Leishmania donovani. *Clinical Infectious Diseases* **72**, e526–e532 (2021).

721 16. Imamura, H. *et al.* Evolutionary genomics of epidemic visceral leishmaniasis in the Indian
722 subcontinent. *Elife* **5**, (2016).

723 17. Dumetz, F. *et al.* Molecular Preadaptation to Antimony Resistance in Leishmania donovani on
724 the Indian Subcontinent. *mSphere* **3**, (2018).

725 18. Downing, T. *et al.* Whole genome sequencing of multiple Leishmania donovani clinical isolates
726 provides insights into population structure and mechanisms of drug resistance. *Genome Res*
727 **21**, 2143–2156 (2011).

728 19. Dumetz, F. *et al.* Modulation of aneuploidy in leishmania donovani during adaptation to
729 different in vitro and in vivo environments and its impact on gene expression. *mBio* **8**, (2017).

730 20. Hefnawy, A. *et al.* Genomic and Phenotypic Characterization of Experimentally Selected
731 Resistant Leishmania donovani Reveals a Role for Dynamin-1-Like Protein in the Mechanism of
732 Resistance to a Novel Antileishmanial Compound. *mBio* **13**, (2022).

733 21. Shaw, C. D. *et al.* In vitro selection of miltefosine resistance in promastigotes of Leishmania
734 donovani from Nepal: genomic and metabolomic characterization. *Mol Microbiol* **99**, 1134–
735 1148 (2016).

736 22. Barrett, M. P., Kyle, D. E., Sibley, L. D., Radke, J. B. & Tarleton, R. L. Protozoan persister-like cells
737 and drug treatment failure. *Nature Reviews Microbiology 2019 17:10* **17**, 607–620 (2019).

738 23. Jara, M. *et al.* Unveiling drug-tolerant and persister-like cells in Leishmania braziliensis lines
739 derived from patients with cutaneous leishmaniasis. *Front Cell Infect Microbiol* **13**, 1253033
740 (2023).

741 24. Jara, M. *et al.* Transcriptional Shift and Metabolic Adaptations during Leishmania Quiescence
742 Using Stationary Phase and Drug Pressure as Models. *Microorganisms* **10**, 97 (2022).

743 25. Kloehn, J. *et al.* Identification of metabolically quiescent leishmania mexicana parasites in
744 peripheral and cured dermal granulomas using stable isotope tracing imaging mass
745 spectrometry. *mBio* **12**, (2021).

746 26. Dirkx, L. *et al.* Long-term hematopoietic stem cells trigger quiescence in Leishmania parasites.
747 *PLoS Pathog* **20**, e1012181 (2024).

748 27. Kloehn, J., Saunders, E. C., O'Callaghan, S., Dagley, M. J. & McConville, M. J. Characterization of
749 Metabolically Quiescent Leishmania Parasites in Murine Lesions Using Heavy Water Labeling.
750 *PLoS Pathog* **11**, e1004683 (2015).

751 28. Mandell, M. A. & Beverley, S. M. Continual renewal and replication of persistent Leishmania
752 major parasites in concomitantly immune hosts. *Proc Natl Acad Sci U S A* **114**, E801–E810
753 (2017).

754 29. Dirkx, L. *et al.* Long-term hematopoietic stem cells as a parasite niche during treatment failure
755 in visceral leishmaniasis. *Communications Biology 2022 5:1* **5**, 1–15 (2022).

756 30. Brotherton, M. C. *et al.* Proteomic and Genomic Analyses of Antimony Resistant Leishmania
757 infantum Mutant. *PLoS One* **8**, e81899 (2013).

758 31. Patino, L. H. *et al.* Major changes in chromosomal somy, gene expression and gene dosage
759 driven by SbIII in Leishmania braziliensis and Leishmania panamensis. *Scientific Reports 2019*
760 *9:1* **9**, 1–13 (2019).

761 32. Negreira, G. H. *et al.* High throughput single-cell genome sequencing gives insights into the
762 generation and evolution of mosaic aneuploidy in Leishmania donovani. *Nucleic Acids Res* **50**,
763 293–305 (2022).

764 33. Sterkers, Y. *et al.* Novel insights into genome plasticity in Eukaryotes: mosaic aneuploidy in
765 Leishmania. *Mol Microbiol* **86**, 15–23 (2012).

766 34. Wyllie, S., Cunningham, M. L. & Fairlamb, A. H. Dual Action of Antimonial Drugs on Thiol Redox
767 Metabolism in the Human Pathogen Leishmania donovani. *Journal of Biological Chemistry*
768 **279**, 39925–39932 (2004).

769 35. Goyard, S. *et al.* An in vitro system for developmental and genetic studies of Leishmania
770 donovani phosphoglycans. *Mol Biochem Parasitol* **130**, 31–42 (2003).

771 36. Jara, M. *et al.* Tracking of quiescence in Leishmania by quantifying the expression of GFP in the
772 ribosomal DNA locus. *Scientific Reports 2019 9:1* **9**, 1–12 (2019).

773 37. Taneja, N. K. & Tyagi, J. S. Resazurin reduction assays for screening of anti-tubercular
774 compounds against dormant and actively growing Mycobacterium tuberculosis,
775 Mycobacterium bovis BCG and Mycobacterium smegmatis. *Journal of Antimicrobial*
776 *Chemotherapy* **60**, 288–293 (2007).

777 38. Chawla, B., Jhingran, A., Panigrahi, A., Stuart, K. D. & Madhubala, R. Paromomycin Affects
778 Translation and Vesicle-Mediated Trafficking as Revealed by Proteomics of Paromomycin –
779 Susceptible –Resistant Leishmania donovani. *PLoS One* **6**, e26660 (2011).

780 39. Rakotomanga, M., Blanc, S., Gaudin, K., Chaminade, P. & Loiseau, P. M. Miltefosine Affects
781 Lipid Metabolism in Leishmania donovani Promastigotes. *Antimicrob Agents Chemother* **51**,
782 1425 (2007).

783 40. Stone, N. R. H., Bicanic, T., Salim, R. & Hope, W. Liposomal Amphotericin B (AmBisome®): A
784 Review of the Pharmacokinetics, Pharmacodynamics, Clinical Experience and Future
785 Directions. *Drugs 2016 76:4* **76**, 485–500 (2016).

41. López-Arencibia, A., Bethencourt-Estrella, C. J., San Nicolás-Hernández, D., Lorenzo-Morales, J. & Piñero, J. E. Anti-COVID Drugs (MMV COVID Box) as Leishmanicidal Agents: Unveiling New Therapeutic Horizons. *Pharmaceuticals* **17**, 266 (2024).

42. Sogbein, O. *et al.* Bortezomib in cancer therapy: Mechanisms, side effects, and future proteasome inhibitors. *Life Sci* **358**, 123125 (2024).

43. Brauner, A., Fridman, O., Gefen, O. & Balaban, N. Q. Distinguishing between resistance, tolerance and persistence to antibiotic treatment. *Nature Reviews Microbiology 2016 14:5* **14**, 320–330 (2016).

44. Balaban, N. Q., Merrin, J., Chait, R., Kowalik, L. & Leibler, S. Bacterial persistence as a phenotypic switch. *Science (1979)* **305**, 1622–1625 (2004).

45. El Fadili, K. *et al.* Role of the ABC transporter MRPA (PGPA) in antimony resistance in Leishmania infantum axenic and intracellular amastigotes. *Antimicrob Agents Chemother* **49**, 1988–1993 (2005).

46. Sun, L. L. *et al.* Aneuploidy enables cross-tolerance to unrelated antifungal drugs in Candida parapsilosis. *Front Microbiol* **14**, 1137083 (2023).

47. Yang, F. *et al.* Aneuploidy Enables Cross-Adaptation to Unrelated Drugs. *Mol Biol Evol* **36**, 1768–1782 (2019).

48. Negreira, G. H. *et al.* The adaptive roles of aneuploidy and polyclonality in Leishmania in response to environmental stress . *EMBO Rep* **24**, (2023).

49. Sterkers, Y., Lachaud, L., Crobu, L., Bastien, P. & Pagès, M. FISH analysis reveals aneuploidy and continual generation of chromosomal mosaicism in Leishmania major. *Cell Microbiol* **13**, 274–283 (2011).

50. Kulshrestha, A. *et al.* Validation of a simple resazurin-based promastigote assay for the routine monitoring of miltefosine susceptibility in clinical isolates of Leishmania donovani. *Parasitol Res* **112**, 825–828 (2013).